FLEXURAL BEHAVIOR OF PROPOSED STEEL-TIMBER-CONCRETE COMPOSITE FLOOR SYSTEMS FOR MID-TO-HIGH-RISE BUILDINGS

Chae-yeon Kim[1], Min-su Kang[2], Jong-soo Choi[3], Jin-won Shin[4], Kyong-soo Yom[5], Sung-mo Choi [6]

ABSTRACT: This study experimentally evaluates the flexural performance of an STC (Steel-Timber-Concrete) slab composed of steel (Z-section), concrete, and CLT, and aims to derive cross-sectional configurations and allowable spans applicable to mid-to-high-rise timber buildings. A total of six specimens were fabricated and tested under a two-point loading setup, comparing flexural stiffness and strength before and after concrete hardening. The results show improved flexural performance with increasing Z-section thickness and rebar diameter, and that STC slabs could achieve an allowable span of up to 6.25 m after concrete hardening. In particular, the STCJZ slab, with its thermal storage effect of concrete and joist reinforcement, showed favorable fire resistance characteristics. This study experimentally demonstrates the practical feasibility of STC slabs as a structural alternative for high-rise timber construction.

KEYWORDS: Flexural behavior, Steel-timber-concrete, Composite floors, Mid-to-high-rise timber buildings

1. INTRODUCTION

Timber structures have gained global attention as a renewable and sustainable construction method, due to their lightweight nature and low carbon emissions. According to Choi Gyu-woong (2022), for buildings of the same scale, concrete structures emit 79.9 tons of CO_2 (4.24 times more than timber structures), and steel prefab structures emit 54.06 tons (2.86 times more), while timber structures emit only 18.8 tons, making a significant contribution to climate change mitigation.

In contrast, the deck plate construction method is predominantly used in domestic high-rise buildings. This method involves high self-weight and necessitates large equipment such as tower cranes, which not only complicates construction but also increases the risk of structural safety accidents. In fact, according to the Korea Occupational Safety and Health Agency (2019), 29.4% of deck plate-related accidents from 2016 to 2019 were due to structural collapses. As a countermeasure against such recurring structural failures and construction risks, the STC composite structure has emerged as an effective alternative. By combining lightweight timber with high-strength steel and concrete, STC slabs can secure the structural performance required for mid-to-high-rise buildings while also ensuring constructability and sustainability.

Accordingly, this study aims to experimentally evaluate the flexural performance of STC slabs utilizing steel and concrete, and to propose optimal cross-sectional shapes and allowable spans suitable for mid-to-high-rise timber construction.

2. THEORETICAL REVIEW OF STC SLAB

2.1 Existing Studies

A study conducted by the Korea Agency for Infrastructure Technology Advancement (KAIA, 2017) proposed a theoretical analytical model for composite panel floor systems combining engineered wood and concrete. The study verified structural integrity and performance through experiments on various types of shear connectors as well as large-scale bending and vibration tests. It was found that the shear strength and ductility of the composite panel varied depending on the anchorage angle and length of the shear connectors, and that applying a concrete layer thicker than 100 mm improved the fundamental natural frequency by approximately 25%.

Mai Quang Khai (2019) experimentally and numerically evaluated the structural performance of hybrid floor systems composed of CLT and concrete. The study confirmed significant differences in load-bearing capacity and ductility depending on the type, angle, and

[1] Chae-yeon Kim, Dept. of architectural engineering, University of Seoul, Seoul, Korea, codus1141@uos.ac.kr
[2] Min-su Kang, Dept. of architectural engineering, University of Seoul, Seoul, Korea, keizea@naver.com
[3] Jong-soo Choi, Dept. of architectural engineering, University of Seoul, Seoul, Korea, cjs@dukshinepc.com
[4] Jin-won Shin, Dept. of architectural engineering, Catholic Kwandong University Seoul, Korea, jshin@cku.ac.kr
[5] Kyong-soo Yom, Engineer, Actpartner Co., Ltd., Korea, ksyom@actpartner.co.kr
[6] Sung-mo Choi, Dept. of architectural engineering, University of Seoul, Seoul, Korea, smc@uos.ac.kr

https://doi.org/10.52202/080513-0192

penetration depth of shear connectors, as well as the thickness of the concrete layer. This research not only provides a theoretical foundation for STC floor systems but also serves as a meaningful precedent by experimentally demonstrating the feasibility of applying such systems in mid-to-high-rise timber buildings.

2.2 Geometry and Characteristics of STC Slab

The STC slab proposed in this study consists of a composite cross-section with concrete positioned at the top and structural CLT (Cross-Laminated Timber) at the bottom. To enable full composite action of the slab, steel components such as Z-section steel, hex bolts, and nails were employed as shear connectors. These connectors serve to increase the stiffness of the joints and prevent failure of the CLT. The CLT and Z-section steel were connected using 6×38 mm wood deck screws, while the CLT and concrete were joined using STS stainless steel hex bolts (M8×70 mm) or nails (Ø3.4×70 mm). The shear connectors were spaced at 200 mm intervals over a length of 800 mm at each end of the slab, and at 300 mm intervals in the central region. Additionally, to prevent cracking the concrete, 6 mm diameter wire mesh was arranged at 150 mm spacing. These details are illustrated in ***Figure 1.***

2.3 Flexural Performance of STC Slab

The material strengths used for the calculation of flexural capacity are presented in ***Table 1.*** The CLT was assigned the material properties corresponding to grade E1 under the limit state design of KS F 2081:2021. For steel, the properties of SS275 specified in KS D 3503 (2018) were used, while SD400 grade was applied for the reinforcement bars. The strength and elastic modulus of the concrete were determined based on a compressive strength of 24 MPa according to KS F 4009 (2024), and the modulus of elasticity was calculated using the formula for normal-weight aggregate concrete from KDS 14 20 10 (2021).

Table 1. List of Material Properties

Material	E, Modulus of elasticity (MPa)	Strength (MPa)	
CLT	11,722	f_t	15.4
Concrete	25,811	f_{ck}	24
Steel (SS275)	200,000	F_y	275
Rebar (D10, D16)	200,000		400

- f_t: Tensile strength
- f_{ck}: Compressive strength of concrete
- F_y: Yield strength

The flexural capacity of the STC slab was calculated by applying the plastic stress distribution method as described in KDS 41 30 20 (2022), which is the Korean standard for composite steel structures. Full composite action was assumed for the members. Plastic behavior was considered for both concrete and steel, while CLT was treated as having only elastic behavior. Due to the low flexural contribution of the CLT in the minor axis direction, crosswise layers were excluded from the strength calculation. The CLT used in this study consists of a 3-ply configuration in which each layer is arranged perpendicularly. Since the middle layer is orthogonal to the principal stress direction, it was excluded from the effective structural section in the analysis. The flexural stiffness and nominal flexural moment of each section are summarized in ***Table 2.***

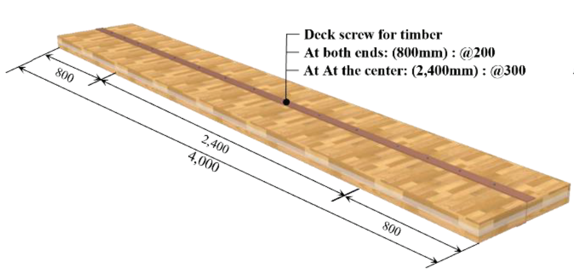

Figure 1.1. CLT-Z section (TZ)

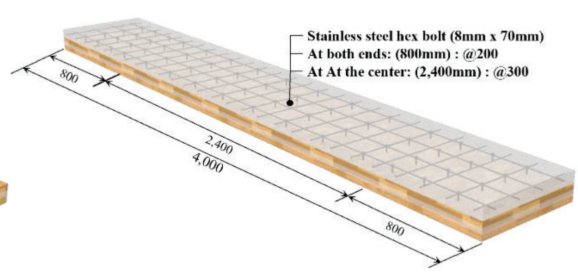

Figure 1.2. Concrete-CLT section (CT)

Figure 1. Connector layout

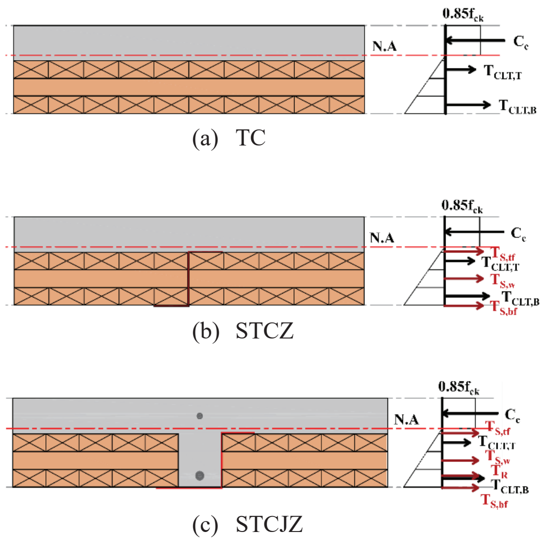

Figure 2. Stress distribution in the composite slabs

$$M_n = T_{CLT,T} \cdot d_{CLT,T} + T_{CLT,B} \cdot d_{CLT,B} + T_{S,tf} \cdot d_{S,tf}$$
$$+T_{S,w} \cdot d_{S,w} + T_{S,bf} \cdot d_{S,bf} + T_R \cdot d_R$$

Where, M_n : Nominal flexural moment
$T_{CLT,T}$: Tensile force in the top layer of the CLT
$d_{CLT,T}$: Distance from the centroid of the top layer tension in CLT to the neutral axis
$T_{CLT,B}$: Tensile force in the bottom layer of the CLT
$D_{CLT,B}$: Distance from the centroid of the bottom layer tension in CLT to the neutral axis
$T_{S,tf}$: Tensile force in the top flange of the Z-section steel
$d_{S,tf}$: Distance from the centroid of the top flange tension in Z-section to the neutral axis
$T_{S,w}$: Tensile force in the web of the Z-section steel
$d_{S,w}$: Distance from the centroid of the web tension in Z-section to the neutral axis
$T_{S,bf}$: Tensile force in the bottom flange of the Z-section steel
$d_{S,bf}$: Distance from the centroid of the bottom flange tension in Z-section to the neutral axis
T_R : Tensile force in the bottom reinforcing bar
d_R : Distance from the centroid of bottom rebar tension to the neutral axis

$$y_C = \frac{A_{Conc} \cdot y_{Conc} + nA_{CLT} \cdot y_{CLT} + n'A_S \cdot y_S}{A_{CLT} + nA_{Conc} + n'A_S}$$

Where, y_C : Position of the neutral axis of the composite section
A_{Conc} : Cross-sectional area of the concrete
A_{CLT} : Cross-sectional area of the CLT
A_S : Cross-sectional area of the steel
y_{Conc} : Distance from the centroid of the concrete to the neutral axis
y_{CLT} : Distance from the centroid of the CLT to the neutral axis
y_S : Distance from the centroid of the steel to the neutral axis
n : Modular ratio between concrete and CLT
n' : Modular ratio between concrete and steel

$$I_C = I_{Conc} + A_{Conc} \cdot (y_C - y_{Conc})^2 + nI_{CLT}$$
$$+ nA_{CLT} \cdot (y_C - y_{CLT})^2 + n'I_S + n'A_S(y_C - y_S)^2$$

Where, I_C : Moment of inertia of the composite section
I_{Conc} : Moment of inertia of the concrete
I_{CLT} : Moment of inertia of the CLT
I_S : Moment of inertia of the steel

Table 2. List of Material Properties.

No.	T	TZ	TC	STCZ	STCZ (Nail)	STCJZ
Flexural stiffness (10^{12}N·mm^2)	0.41	0.63	2.64	3.28	3.28	4.46
	Ratio					
	1.00	0.02	0.08			
			1.00	0.10	0.10	0.13
Flexural strength (kN·m/m)	13.86	20.75	47.66	51.41	51.41	58.91
	Ratio					
	1.00	0.55	0.27			
			1.00	1.14	1.14	1.31

3. Flexural Behavior Experiment of STC Slab

3.1 Overview

The flexural behavior of the STC slab was evaluated through a two-point loading test using a Universal Testing Machine (UTM). The total length of the specimen was 4000 mm, with a span of 3600 mm between supports. The load was applied at the third-span points. The reference specimen consisted of a three-layer CLT panel (600 × 90 × 4000 mm), and six different cross-sectional configurations were tested by varying the inclusion of Z-section steel, concrete, and joists.

https://doi.org/10.52202/080513-0192

3.2 Plan and Method

The cross-sectional configurations and key experimental variables are summarized in ***Table 3.*** The primary variables included the presence or absence of Z-section steel, concrete, and joists. Strain gauges were attached starting 15 mm above the bottom surface of the specimens, at vertical intervals of 30 mm. They were installed at the mid-width of the specimens and 30 mm inward from both ends. For the Z-section steel, strain gauges were placed at the midpoints of the top, middle, and bottom regions. In the STCJZ configuration, additional gauges were attached to the bottom reinforcing bars to monitor the composite behavior more precisely. The layout of the strain gauges is illustrated in ***Figure 4.***

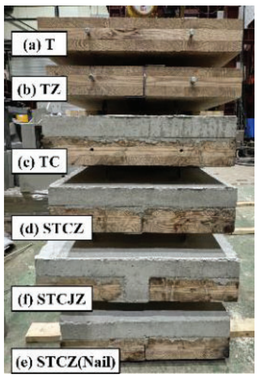

Figure 3.1 Cross-section of each specimen

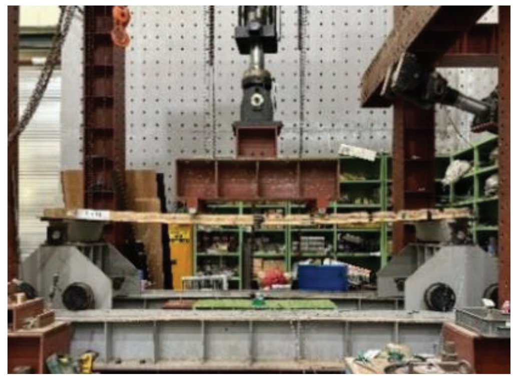

Figure 3.2 Universal Testing Machine (UTM)

Figure 3. Test Equipment and Specimens

Table 3. List of each specimen

Specimen	(a) T	(b) TZ	(c) TC
Section	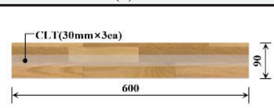	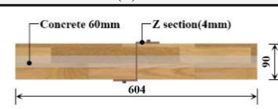	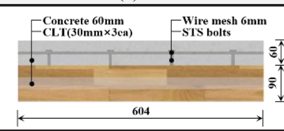
CLT	600×90×4000 (30×3ea)	300×90×4000 (30×3ea), 2ea	600×90×4000 (30×3ea)
Z section	-	94×60×60, 4T (SS275)	-
Specimen	(d) STCZ	(e) STCZ (Nail)	(f) STCJZ
Section	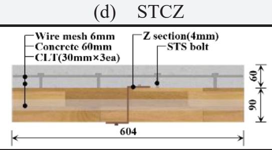	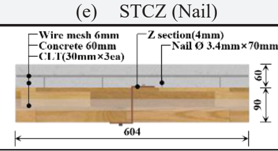	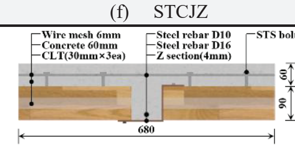
CLT	300×90×4000 (30×3ea), 2ea		
Z section	94×60×60, 4T (SS275)		94×60×120, 4T (SS275)

- S : Steel
- T : CLT(Cross-Laminated Tmber)
- C : Concrete
- J : Joist
- Z : Z section
- Steel rebar : D16, D10
- Wire mesh : 6mm @150mm
- STS Bolt : M8×70mm, M8×30mm
- Nail : ø 3.4mm×70mm

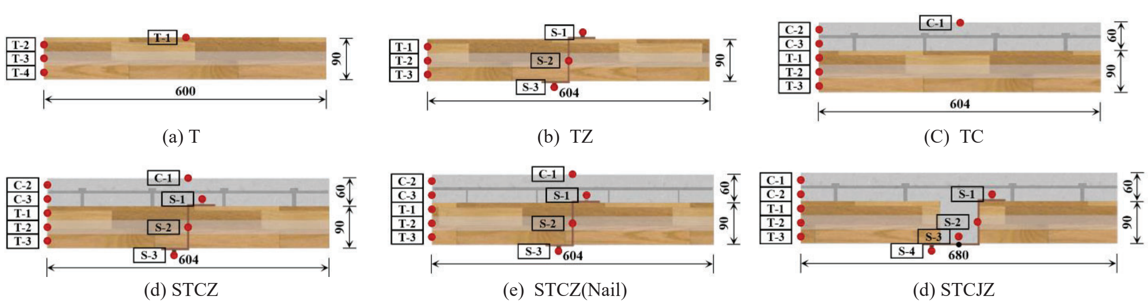

Figure 4. Strain gauge locations of each specimen.

3.3 Results

The load–displacement curves for each specimen are presented in ***Figure 5.***, and the test data are summarized in ***Table 4.*** The yield load F_y was derived using the 1/3 tangent method specified in EN 12512 (2001), and the load at which rapid deformation begins during tensile failure of the timber was defined as F_y', or 80% of the peak load. The deflection limit, F_{dl} was set to L/400, where L is the span length between the two supports.

Specimen (a), composed of pure CLT, exhibited clear elastic behaviours but failed in a brittle manner after reaching peak load, accompanied by a sudden drop in the load. All other specimens showed plastic behaviours after yielding, and even after tensile failure of the timber, the reinforcements shared the tensile force, enabling the specimen to continue bearing load.

In specimen (b) TZ, the strain gauge was improperly attached, and partial detachment of the member occurred, resulting in unreliable data. However, aside from (b), all specimens demonstrated the contribution of the reinforcement to structural performance. The TC specimen (c), which added concrete and used STS hex bolts as shear connectors, showed a 1.2% increase in peak load compared to (a) T. The STCZ specimen (d), with additional Z-section reinforcement, demonstrated a 1.73% increase in peak load over (c), indicating improved flexural stiffness.

Specimen (e) STCZ (Nail), structurally identical to (d) but using nails instead of bolts as shear connectors, exhibited a peak load of 72.50 kN, about 6.8% lower than that of (d). This result suggests that nails offer lower shear resistance, which diminishes the composite effect between CLT and concrete, while STS hex bolts more effectively enhance shear resistance. The STCJZ specimen (f) showed the highest peak load at 106.50 kN, representing a 2.37% increase over (c) TC. This improvement is attributed to the combined reinforcement of Z-section steel and joists, as well as sufficient shear resistance provided by the STS hex bolts.

Analysis of the load–strain curves revealed that the neutral axis shifted upward as the load increased. Even after the fracture of the timber, the steel reinforcement in the STCJZ specimen retained residual strength, allowing for stress redistribution. This behavior demonstrates the influence of the difference in elastic moduli between steel and timber on the movement of the neutral axis and stress transfer, as shown in ***Figure 6.***

Strain distributions in both the compression and tension zones indicated that the entire cross-section approached near-plastic behavior. As the span-to-depth ratio increased, all specimens exhibited greater deflection, and when the ratio exceeded 25, distinct differences in deflection among materials became apparent. This highlights the increasing effect of material stiffness on deflection under larger span conditions, as illustrated in ***Figure 7***.

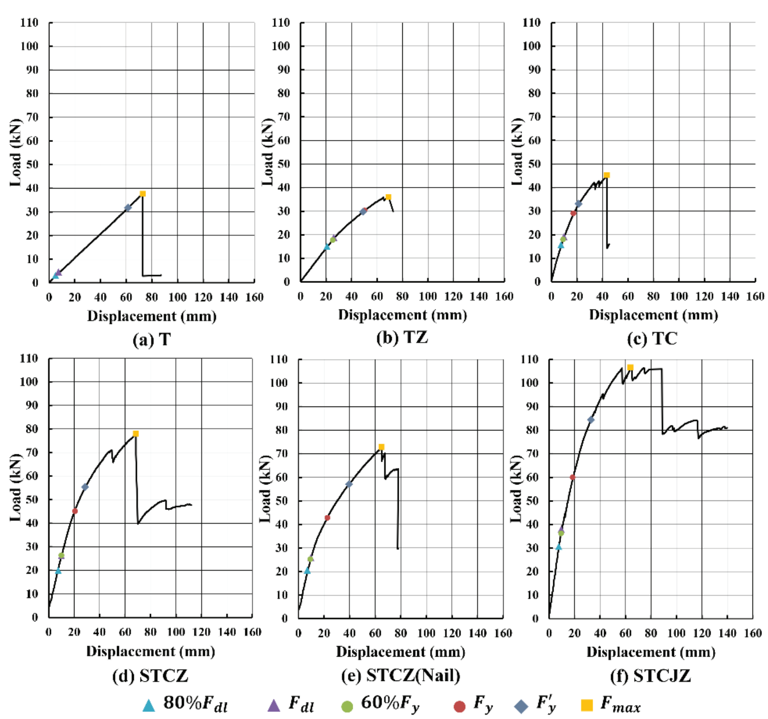

Figure 5. Load–span deflection curves for each group of specimens.

https://doi.org/10.52202/080513-0192

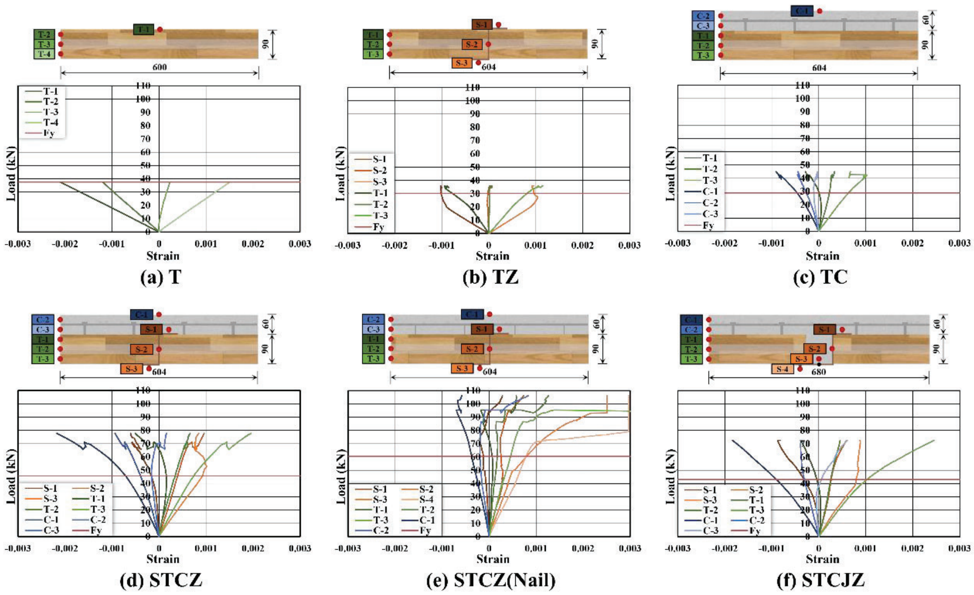

Figure 6. Strain development curves for each group of specimens.

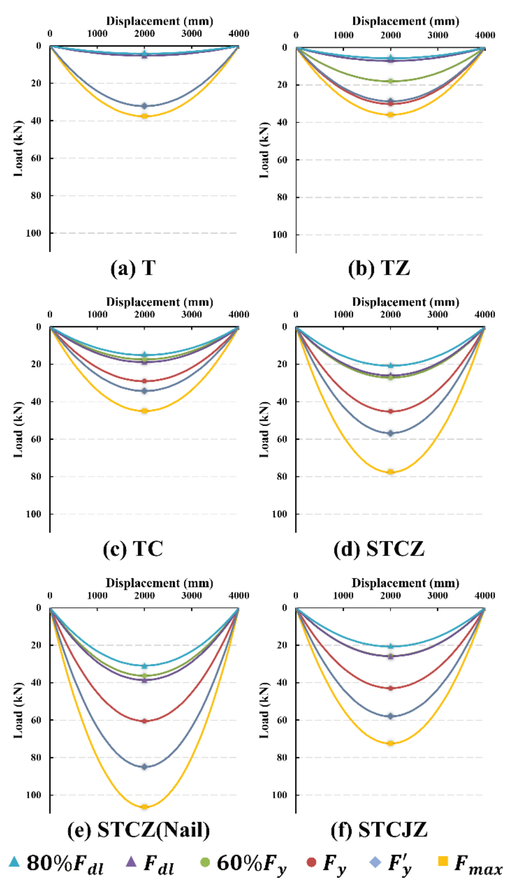

Figure 7. Deflection development curves for each specimen group.

No. / Load (kN)	(a) T	(b) TZ	(c) TC	(d) STCZ	(e) STCZ (Nail)	(f) STCJZ
80%F_{dl}	4.21	5.73	15.12	20.80	20.72	30.88
F_{dl}	5.26	7.17	18.90	26.00	25.90	38.60
60%F_y	-	18.09	17.43	27.16	25.75	36.30
F_y	-	30.15	29.05	45.26	42.91	60.50
$F_y{'}$	32.20	28.73	33.28	56.80	58.00	85.04
	Ratio					
	1.00	0.89	1.03			
			1.00	1.71	1.74	2.56
F_{max}	37.64	35.92	45.00	77.80	72.50	106.50
	Ratio					
	1.00	0.95	1.20			
			1.00	1.73	1.61	2.37

- F_{dl}: Load at the deflection limit (L/400)
- F_y: Yield load determined by the 1/3 tangent method (EN 12512)
- $F_y{'}$: Experimentally determined yield load
- F_{max}: Peak load

Table 4. Test data for each group of specimens

4. DISCUSSION ON ALLOWABLE SPAN AND FLEXURAL BEHAVIOR OF THE PROPOSED STC SLABS

4.1 Flexural Stiffness and Strength Before Concrete Hardening

The flexural stiffness and flexural strength of each slab type at the time of concrete casting are presented in **Table 5.** Taking the TC slab as a reference, the STCZ slabs showed gradual improvement in flexural performance as the thickness of the JZ-section increased. Notably, when the

Z-section thickness reached 6 mm, the flexural stiffness and strength increased by approximately 2.29 and 2.22 times, respectively, compared to the TC slab. In contrast, the STCJZ slab exhibited consistent flexural stiffness (1.46 times that of TC), while its strength slightly increased from 1.22 to 1.30 times as the rebar diameter changed from D10 to D19. This suggests that rebar contributes minimally to structural performance before concrete hardening.

Table 5. Test data for each group of specimens

	TC	STCZ			STCJZ		
		2mm	4mm	6mm	D10	D16	D19
Flexural stiffness (10^{12}N·mm^2)	0.41	0.55	0.73	0.94	0.60	0.60	0.60
	Ratio						
	1.00	1.34	1.77	2.29	1.46	1.46	1.46
Flexural strength (kN·m/m)	15.02	20.46	26.55	33.36	18.29	19.06	19.58
	Ratio						
	1.00	1.36	1.77	2.22	1.22	1.27	1.30

4.2 Flexural Stiffness and Strength After Concrete Hardening

After the concrete hardened, all slab types exhibited significant improvement in flexural performance. In the STCZ slabs, both flexural stiffness and strength continued to increase with the thickness of the Z-section. With a 6 mm Z-section, the flexural stiffness and strength were improved by approximately 1.38 and 1.83 times, respectively, compared to the TC slab. For the STCJZ slab, flexural strength clearly increased with rebar diameter, showing about a 1.63-fold increase with D19 compared to D10. This confirms that rebar plays a significant structural role after concrete hardening and greatly influences the behaviours of the composite section.

Table 6. Test data for each group of specimens

	TC	STCZ			STCJZ		
		2mm	4mm	6mm	D10	D16	D19
Flexural stiffness (10^{12}N·mm^2)	2.32	2.66	2.99	3.20	3.06	3.17	3.23
	Ratio						
	1.00	1.15	1.29	1.38	1.32	1.37	1.39
Flexural strength (kN·m/m)	30.59	39.47	47.86	56.07	42.54	46.98	49.88
	Ratio						
	1.00	1.29	1.56	1.83	1.39	1.54	1.63

4.3 Allowable Span of STC Slabs

The allowable span was calculated based on a working load of 2.5 kN/m² during concrete casting and a live load of 5.0 kN/m² after hardening, corresponding to standard use loads in residential common areas. As a result, the TC slab was capable of spanning approximately 3.33 m during casting. In comparison, the STCZ slabs, with Z-section thicknesses ranging from 2 mm to 6 mm, achieved allowable spans from 4.02 m to 4.75 m, indicating suitability for high-rise structures requiring longer spans. The STCJZ slab showed a consistent allowable span of 3.91 m during casting regardless of rebar diameter. After hardening, the allowable span increased for all slabs, with STCZ reaching up to 6.25 m and STCJZ up to 6.01 m. In particular, the STCJZ slab benefits from the thermal storage capacity of concrete, which enhances fire resistance.

Table 7. Test data for each group of specimens

	TC	STCZ			STCJZ		
		2mm	4mm	6mm	D10	D16	D19
during concrete pouring (m)	3.33	4.02	4.38	4.75	3.91	3.91	3.91
after conc. hardening (m)	5.63	5.86	6.07	6.25	5.91	5.98	6.01

5. SUMMARIES

This study proposes an STC hybrid floor system composed of Z-section steel, concrete, and CLT, and evaluates its flexural performance through experimental testing. The key findings are summarized as follows:

1) The pure CLT slab exhibited brittle failure after reaching peak load. In contrast, STC slabs reinforced with Z-section steel, concrete, and rebar demonstrated plastic behaviours, retaining residual strength even after yielding. In particular, the STCJZ slab showed a 2.37-fold increase in maximum load compared to the TC slab, due to the combined effects of Z-section and joist reinforcement. Stress redistribution and upward movement of the neutral axis were also observed under increasing load.

2) At the time of concrete casting, the STCZ slab showed improved flexural performance with increasing Z-section thickness. With a 6 mm Z-section, the flexural stiffness and strength increased by approximately 2.29 and 2.22 times, respectively, compared to the TC slab. The STCJZ slab demonstrated similar performance regardless of rebar diameter, suggesting that rebar contributes little before hardening.

3) After concrete hardening, all slab types exhibited marked improvements in flexural performance. The STCZ slab continued to show performance

https://doi.org/10.52202/080513-0192

gains with increased Z-section thickness, and the STCJZ slab showed a 1.63-fold increase in flexural strength when using D19 instead of D10, highlighting the structural significance of rebar after hardening.

4) In terms of allowable span, the TC slab achieved approximately 3.33 m during casting. The STCZ slab showed improved spans up to 4.75 m depending on Z-section thickness. After concrete hardening, allowable spans increased to 6.25 m for STCZ and 6.01 m for STCJZ. The STCJZ slab demonstrated favourable structural characteristics for fire resistance due to the thermal mass of concrete.

6. REFERENCES

[1] Choi, Gyu-woong (2020), A Study on the Application of Domestic Softwood Ply-Lam CLT as Beam Members in Timber Buildings. PhD diss., Graduate School, Chungnam National University, Daejeon, Korea.

[2] European Committee for Standardization, Eurocod 3: Design of steel structures-Part 1-2: General rules-Structural fire design (EN 1993-1-2:2005), April 2005.

[3] European Committee for Standardization, Timber Structures – Test Methods – Cyclic Testing of Joints Made with Mechanical Fasteners (EN 12512:2001), April 2005.

[4] Gwak, J. Y. (2025), Fire Resistance Performance of Steel-Timber-Concrete Composite Slabs Exposed to Standard Fire. University of Seoul.

[5] Khai, M.Q. (2019), Structural performance evaluation of the hybrid cross laminated timber, Doctoral dissertation, Sejong University, Seoul.

[6] Korea Agency for Infrastructure Technology Advancement (2017), Development of composite panel floor system using engineered wood and concrete, National Library of Korea, https://www.nl.go.kr/NL/contents/search.do?

[7] Korean Industrial Standards Council, KS F 2257-1:2019 Fire resistance test methods for building components - General requirements, KOREAN STANDARD & CERTIFICATION, Amended in 2019, https://standard.go.kr/

[8] The Engineered Wood Association. (2025). *ANSI/APA PRG 320-2025: Standard for performance-rated cross-laminated timber*. American National Standards Institute. https://www.apawood.org

[9] Zhang, A., Chen, Z., & Liu, J. (2024), Flexural performance of innovative thin-walled steel–timber composite floor slabs, *Engineering Structures*, vol. 318, Article no. 118676, https://doi.org/10.1016/j.engstruct.2024.118676

ACKNOWLEDGMENT

This research was supported by the National Research Foundation of Korea (RS-2023-00273519) with funding from the Ministry of Science and ICT.